A model of three coupled wave guides and third order exceptional points

W D Heiss[1,2], G Wunner[3],

[1]Department of Physics, University of Stellenbosch, 7602 Matieland, South Africa
[2]National Institute for Theoretical Physics (NITheP), Western Cape, South Africa
[3]Institut für Theoretische Physik, Universität Stuttgart, Pfaffenwaldring 57, 70 569 Stuttgart, Germany

E-mail: dieter@physics.sun.za

E-mail: wunner@itp1.uni-stuttgart.de

Abstract. A $\mathcal{PT}$-symmetric model for three interacting wave guides is investigated. Each wave guide is represented by an attractive δ-function potential being in equidistant positions. The two outer potentials are complex describing loss and gain, respectively. The real parts of the outer potentials are assumed to be equal. The major focus of the study lies on the occurrence of an exceptional point of third order and the physical effects of such singularity. While some results resemble those from similar studies with two wave guides, the three wave guides appear to have a richer structure. Emphasis is placed on the fine tuning in the approach of the EP3 as this appears to be a particular challenge for an experimental realization.

PACS numbers: 42.50.Xa, 03.65.Ge, 02.40.Xx

Submitted to: *J. Phys. A: Math. Gen.*

1. Introduction

Exceptional points are points in the parameter space of a physical system where both eigenvalues and eigenvectors coincide. They can occur only for non-hermitian operators. Exceptional points appear in particular in $\mathcal{PT}$-symmetric systems which are symmetric under the combined action of parity inversion and time reversal. In a ground-breaking paper in 1998 Bender and Boettcher [1] demonstrated that $\mathcal{PT}$-symmetric non-hermitian Hamiltonians can have real eigenvalues, and that eigenstates coalesce at exceptional points when the symmetry is broken. Since then there has been a host of papers discussing $\mathcal{PT}$ symmetry in a diversity of physical systems, involving microwave cavities, superconductivity, atomic diffusion, nuclear magnetic resonance, coupled classical and electronic oscillators, and in particular in optics (see, e. g., [2–4] and references therein).

In a seminal paper in 2008, Klaiman et al. [5] proposed the experimental visualization of exceptional points of second order in a system of two coupled $\mathcal{PT}$-symmetric wave guides. Their model consists of two wave guides in which the refractive index differs from that of the background substrate (n_0) by a small amount Δn, and imaginary parts $\pm\gamma$ of equal size but opposite sign are introduced in the guides. Their predictions received convincing confirmation 2010 in the experiment by Rüter et al. [6], when the coalescence of two wave guide modes at a branch point of second order was observed, when gain and loss were increased up to a critical value. In the experiment, loss is realized by pasting a metal on one wave guide, and gain by pumping laser light on the other.

The present paper goes beyond these investigations and explores the possibility of observing exceptional points of higher order, i.e. the coalescence of more than two modes in multi wave guide systems. Specifically, as a natural next step we consider a $\mathcal{PT}$ triple wave guide system and search for the physical conditions under which an exceptional point of third order (EP3) could be observed. The effects of exceptional points of higher order in particular of third order (EP3s), have received increasing attention in recent years [7–15]. Extending the model by Klaiman et al. [5] we place a third wave guide between the guides with gain and loss, but with only a real part of the refractive index that may be different from that of the outer wave guides.

We make use of the formal analogy between the equation of electrodynamics in paraxial approximation governing the propagation of waves and the one-dimensional Schrödinger equation of quantum mechanics. In this analogy the propagation direction of the waves (usually the z direction) is supplanted by time, and the refractive index $n(x)$ is replaced by the potential $V(x) = -k_0^2 n^2(x)$, where k_0 is the vacuum wave number. Thus the equivalent quantum mechanical problem is that of two potential wells of equal depth and the same amount of gain in one and loss in the other, and a third well with only a real-valued potential of different depth between them.

To gain insight we simplify the problem further and model the potential wells by three delta functions. Delta-function potentials are popular as model systems in the literature [16–24], since they allow for analytic or partially analytic solutions, but are flexible enough to provide insight into characteristic phenomena of the more complex physical situations. Our model is expected to capture the essential features of the real, i.e. experimental problem, and may serve as a guide for the search of higher exceptional points in real multi wave guide systems. In fact, our findings point to high sensitivity in the parameters near to the EP3. In particular it is argued that, in contrast to the case of an EP2, a close approach of an EP3 cannot be achieved

with only one real parameter. We hope that our findings can serve as a guide in an experimental effort to show that an EP3 is a physical reality.

2. The model for three wave guides

We model a $\mathcal{PT}$-symmetric system of three coupled wave guides by three delta-function shaped potential wells located at $x = \pm b$ and $x = 0$, where loss is added to the left well while the same amount of gain is added to the right well. The connection to realistic wave guides is established in Appendix C. The corresponding Schrödinger equation used in the present paper reads:

$$\begin{aligned} -\Psi''(x) - & \left[(1+i\gamma)\delta(x+b) + \Gamma\delta(x) + (1-i\gamma)\delta(x-b)\right]\Psi(x) \\ & = -k^2\Psi(x)\,. \end{aligned} \tag{1}$$

The real-valued parameter γ determines the strength of the gain and loss terms. Units have been chosen in such a way that the strength of the real part of the two outer delta-function potentials is normalized to unity, while in the middle well we allow for a different depth given by the the real parameter $\Gamma > 0$. For stationary solutions the eigenvalues k are real, but since the complete eigenvalue spectrum is complex in general, we will also consider solutions with $k \in \mathbb{C}$, $\mathrm{Re}(k) > 0$. Yet our major emphasis is focused upon the bound state solutions with real eigenvalues.

The bound-state wave function has the form (see also Appendix A):

$$\Psi(x) = \begin{cases} A\,\mathrm{e}^{kx} & : \quad x < -b \\ 2\,(r\cosh(kx) + \varrho_1 \sinh(kx)) & : \quad -b < x < 0 \\ 2\,(r\cosh(kx) + \varrho_2 \sinh(kx)) & : \quad 0 < x < b \\ B\,\mathrm{e}^{-kx} & : \quad b < x \end{cases}$$

Applying at the delta functions the continuity conditions for the wave functions and the discontinuity conditions for their first derivatives we obtain the system of linear equations for three unknowns

$$\mathcal{M}\begin{pmatrix} r \\ \varrho_1 \\ \varrho_2 \end{pmatrix} = \begin{pmatrix} 0 \\ 0 \\ 0 \end{pmatrix} \tag{2}$$

with the matrix

$$\mathcal{M} = \begin{pmatrix} \kappa_0 \mathrm{e}^{-2kb} + \kappa_0 - 2k & \kappa_0 \mathrm{e}^{-2kb} - \kappa_0 + 2k & 0 \\ \kappa_0^* \mathrm{e}^{-2kb} + \kappa_0^* - 2k & 0 & -\kappa_0^* \mathrm{e}^{-2kb} + \kappa_0^* - 2k \\ -\Gamma & k & -k \end{pmatrix} \tag{3}$$

where $\kappa_0 = 1 + i\gamma$. The remaining coefficients A and B are related to r, ϱ_1, ϱ_2 by $A = r(1+\mathrm{e}^{2kb}) + \varrho_1(1-\mathrm{e}^{2kb})$, $B = r(1+\mathrm{e}^{2kb}) + \varrho_2(\mathrm{e}^{2kb}-1)$.

The eigenvalues k are obtained by finding the roots of the corresponding secular equation

$$\begin{aligned} \det(\mathcal{M}) = & \\ \Gamma\Big(\mathrm{e}^{-4kb}(1+\gamma^2) & - 2\mathrm{e}^{-2kb}(\gamma^2 - 2k + 1) + \gamma^2 + (2k-1)^2\Big) + \\ +2k\Big(\mathrm{e}^{-4kb}(1+\gamma^2) & - \gamma^2 - (2k-1)^2\Big) = 0\,. \end{aligned} \tag{4}$$

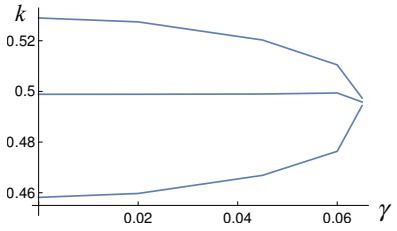

Figure 1. Eigenvalues k for a few points chosen of γ of the three bound states of the underlying model for $b = 6.1$; of course the curves are smooth for a continuous variation of the parameters. Note that close to the exceptional point where the three eigenvalues would coalesce the distance has to be adjusted to $b = 6.2075$ (see text).

The roots depend on three parameters, the distance b of the wells, the strength γ of the loss/gain terms, and the depth Γ of the middle well.

It is instructive to consider the limit $kb \gg 1$, i. e., no coupling between the modes. Then (4) simplifies to

$$\left[\gamma^2 + (2k-1)^2\right](\Gamma - 2k) = 0 \tag{5}$$

with the solutions $k_1 = \Gamma/2$ and $k_{2,3} = (1 \pm i\gamma)/2$. This means that the middle well retains its unperturbed eigenvalue, while the eigenvalues of the outer wells acquire an imaginary part, corresponding to the exponential growth and decrease of the gain and loss mode, respectively. This demonstrates that $\mathcal{PT}$ symmetric modes can exist only when there is sufficient coupling between the wave guides.

Within the present context the case $\gamma = 0$ requires special treatment for the eigenvector of the intermediate (in size), i.e. second eigenvalue k_2. In fact, the explicit values for $\varrho_{1,2}^{(2)}$ obtained for $\gamma > 0$ blow up when $\gamma \to 0$ (see Appendix B). It is related to the fact that in the limit $\gamma \to 0$, the determinant of $\mathcal{M}$ (see (4)) factorizes as

$$(\mathrm{e}^{-2kb} + 2k - 1)\left(\Gamma(\mathrm{e}^{-2kb} + 2k - 1) + 2k(\mathrm{e}^{-2kb} - 2k + 1)\right) = 0\,, \tag{6}$$

which for the second root implies $\mathrm{e}^{-2k_2 b} + 2k_2 - 1 = 0$. Note that this second eigenvalue – yielding the relation $b = -\mathrm{Log}(1-2k_2)/(2k_2)$ – is independent of Γ. Inserting this expression for b into that for $\varrho_{1,2}^{(2)}$ we obtain the expansion

$$\varrho_{1,2}^{(2)} = -i\frac{1-2k_2}{\gamma\, k_2} \pm \frac{1-k_2}{k_2} + O(\gamma)^2 \tag{7}$$

and hence

$$\lim_{\gamma\to 0} \gamma\ \varrho_{1,2}^{(2)} = -i\frac{1-2k_2}{k_2} \tag{8}$$

from which follows

$$\lim_{\gamma\to 0} \gamma \begin{pmatrix} r \\ \varrho_1^{(2)} \\ \varrho_2^{(2)} \end{pmatrix} = -i\frac{1-2k_2}{k_2} \begin{pmatrix} 0 \\ 1 \\ 1 \end{pmatrix}. \tag{9}$$

The essential finding is the factor $-i$ for this second eigenvector in the limit $\gamma \to 0$. As we see in the following section it is due to this factor that we obtain a smooth dependence on γ also for the eigenvector associated with the second eigenvalue.

3. Results and Discussion

3.1. Eigenvalues

For $\gamma = 0$ the model is hermitian, i.e. we expect three real eigenvalues. Owing to the underlying $\mathcal{PT}$ symmetry we expect real eigenvalues for some range $\gamma > 0$ until we reach a coalescence of at least two eigenvalues where two eigenvalues become complex at an EP2. Such value depends on the other parameters b and Γ. Here we seek these parameters in such a way that the triplet of the three (real) parameters (γ, b, Γ) leads to the coalescence of all three levels, i.e. to an EP3.
Let us recall that if a non-hermitian Hamiltonian has an EP3 at a real eigenvalue a change of only one parameter would result in the sprouting out of three coalescing eigenvalues in a symmetric way meaning that at most one eigenvalue can be real while the other two will be complex. In other words, to achieve the coalescence of three real eigenvalues at least two parameters have to be judiciously chosen. It is at this point where we would expect the need for a careful fine-tuning in an experimental realization.

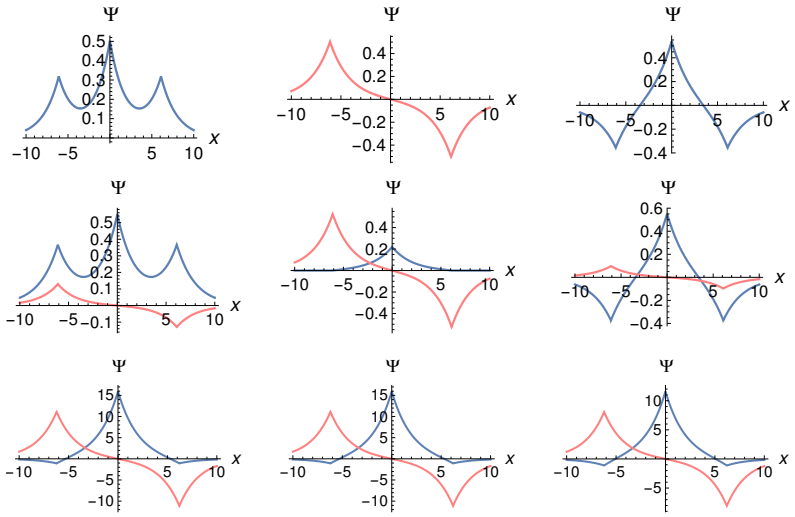

Figure 2. C-normalized wave functions (see text) of the bound states of the underlying model for increasing non-hermiticity parameter (from top to bottom) $\gamma = 0$, 0.02 and 0.065, blue and red illustrate real and imaginary parts, respectively. The rows correspond to decreasing eigenvalues from left to right. The distance between the wells in the two upper panels is $b = 6.1$, while in the bottom panel, close to the EP3, it is $b = 6.2075$. Note the cusps arising from the $\delta-$functions

.

In Fig.1 a set of three eigenvalues is illustrated as a function of γ for $b = 6.1$ and $\Gamma = 1.002$; they are given by the roots of $\det(\mathcal{M})$ (see (4)). Note that the second eigenvalue is almost unaffected by the variation of γ while the other two eigenvalues show a rather weak dependence except for the immediate neighbourhood of the EP3; the illustration stops short of the EP3. The weak dependence on γ of the eigenvalues – except within the near neighbourhood of the EP3 – is due to the fairly large value of b: the states interact weakly away from the singularity. For the

whole interval $0 \leq \gamma \leq 0.06$ the distance between the δ-functions is $b = 6.1$. In line with the previous paragraph we had to re-adjust to $b = 6.2075$ for $\gamma = 0.065$ to ensure real eigenvalues. Had we chosen this value for b also for $\gamma \leq 0.06$ an EP2, i.e. a coalescence of two pairs or complex eigenvalues would have resulted. The values at the EP3 are $\gamma = 0.065278$, $b = 6.20124$, $k = 0.495849$ for $\Gamma = 1.002$. The verification of the EP3 can be achieved numerically: (1) use for the values γ and Γ the values just given at the EP3 and find the (complex) zeros for a first round with $b = 6.20124 + 0.00001 \exp(2i\pi n/50)$ for $n = 0, \ldots, 50$ to obtain the first third of a (possibly slightly deformed) circle around k_{EP3} with a suitable initial value for k, (2) to obtain the second and third section of the closed curve around k_{EP3} use the same procedure with judiciously chosen initial values for k. This way one obtains the full encircling in the $k-$plane by going three times around b_{EP3} in the $b-$plane.

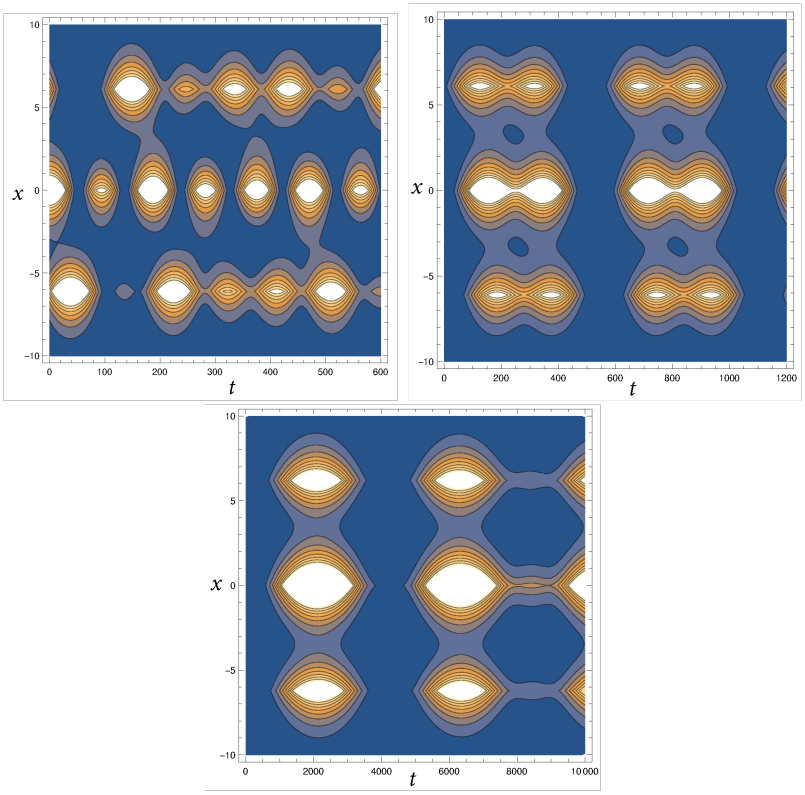

Figure 3. Temporal evolution of a superposition of the three stationary solutions for increasing non-hermiticity parameter. Top left: $\gamma = 0, b = 6.1$, height of contour lines from 0.6 to 0.1, top right: $\gamma = 0.06, b = 6.1$, height of contour lines from 9 to 1, bottom: $\gamma = 0.65, b = 6.2075$, close to the EP3, height of contour lines from 16000 to 2000.

3.2. Wave functions

Some wave functions are illustrated for a few values of γ in Fig.2. The continuous change is clearly visible when γ is switched on. For real eigenvalues, in line with the underlying $\mathcal{PT}$-symmetry, the real part of the wave function must be symmetric and

the imaginary part accordingly antisymmetric. This is the case when the factor $-i$ is applied as discussed at the end of section 2. Note the increasing imaginary part of the wave functions associated with the largest and smallest eigenvalues for increasing γ while it is the real part that is increasing for the intermediate eigenvalue. Near to the EP3 the wave functions become essentially equal as expected. Since we deal with a non-hermitian Hamiltonian we must use the c-norm given by $\langle\tilde{\Psi}|\Psi\rangle$ (with $\langle\tilde{\Psi}|$ being *not* the complex conjugate of $|\Psi\rangle$ but, in this case, rather its equal). Also note that the norms, when taken separately for the real and imaginary part, become comparable for $\gamma \approx \gamma_{EP3}$; in fact their respective c-norms (being the difference of the respective separate norms) vanish at the EP3 as can be noticed by the increasing scale of the wave function.

3.3. Time evolution

The time evolution of the wave functions is given by

$$|\Psi(t,x)\rangle = \sum_{i=1}^{3} c_i \frac{|\Psi_i(x)\rangle}{\langle\tilde{\Psi}_i|\Psi_i\rangle} \exp(i\, k_i^2\, t) \tag{10}$$

with $c_i = \langle\tilde{\Psi}_i|\Psi(t=0)\rangle$ determining an initial condition. Note that here the c-norm is of utmost importance. The modulus squared of (10) yields the intensity within the respective potential wells as a function of t and x. The illustration in Fig.3 displays the results for different parameter sets.

Note the different time scales. Also note the different scales of the heights of the contours owing to the decreasing c-norm. What becomes immediately obvious is the increase of the repeat time of the maxima with increasing γ. Note that we cannot expect strict periodicity as the three eigenvalues are likely to be incommensurate. What is observed here is the beat produced by the three eigenenergies. They are fairly distant for $\gamma = 0$ yielding a short beat time. In contrast, they are very near to each other for $\gamma = 0.065$ yielding a very long beat time. Except for $\gamma = 0$ the pattern is virtually independent of some initial conditions: the system has 'its own life', irrespective of the way it is triggered. This aspect is particularly pronounced in the vicinity of the singularity. We mention that very close to the EP3 the detailed pattern depends somewhat on the path in the two parameter plane by which the EP3 is approached while the gross features prevail.

For different choices of b and Γ an EP3 can be found up to $\Gamma = 1.11$, see Fig. 4. For values of $\Gamma > 1.002$, γ_{EP3} becomes larger while b_{EP3} becomes smaller. However, the qualitative patterns remain similar in that substantial changes happen only close to the EP3. For small values of b (and $\gamma \ll \gamma_{EP3}$), the levels are rather distant due to the stronger coupling. This is why a larger value of γ is needed to force the three levels together. But again, the levels depend weakly on the increasing γ, that is Figs.1-3 remain qualitatively unchanged. The very first point in Figure 4 is for $\Gamma = 1.000001$ as, by the discussion at the end of Section 2, b_{EP3} tends to infinity for $\Gamma \to 1$.

4. Summary and outlook

Using a simple $\mathcal{PT}$-symmetric model for the interaction of three wave guides an exceptional point of third order can be identified for a certain parameter range. Some of the features found are qualitatively reminiscent of similar investigations for two interacting wave guides and an EP of second order. The time dependent pattern

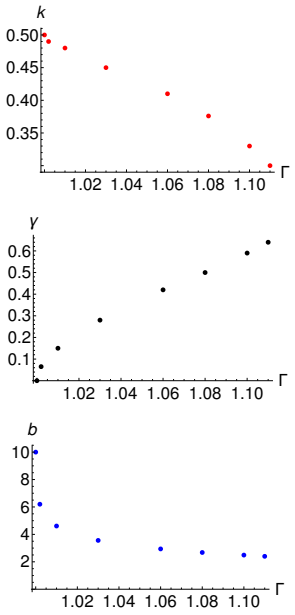

Figure 4. Values of k_{EP3} (top) with the corresponding values for γ_{EP3} (middle) and b_{EP3} (bottom) as a function of Γ. The respective values of the second point in each diagram has been discussed in detail in this paper. The very first point is for $\Gamma = 1.000001$, see text.

(being actually the mode pattern along the extension of the wave guides) shows the characteristic pattern of more and more distant intensity maxima when the spectral singularity is approached.

The new aspect of the present paper is the much increased sensitivity of parameter dependence in the approach of the EP3. Moreover, in the close approach of the EP3 the three eigenvalues cannot be real if only one real parameter is tentatively used. In fact, if an experiment would be attempted with only one parameter two of the three closely lying eigenvalues would infallibly form an EP2 and then disappear into the complex plane. In other words, at least two parameters must be tuned carefully to force three *real* eigenvalues into an EP3 and thus visualize the expected pattern. While this constitutes a great challenge for experimentation we feel that the present paper could give some guidance.

Along this line, an experimental verification of an EP of even higher order would be accordingly more demanding.

Appendix A. Wave function

The bound-state wave function in between the wave guides is a superposition of exponentials

$$\Psi(x) = \begin{cases} C\,\mathrm{e}^{kx} + D\,\mathrm{e}^{-kx} & : \quad -b < x < 0 \\ E\,\mathrm{e}^{kx} + F\,\mathrm{e}^{-kx} & : \quad 0 < x < b \end{cases}$$

If we define $r_1 = (C + D)/2$, $\varrho_1 = (C - D)/2$, $r_2 = (E + F)/2$, $\varrho_2 = (E - F)/2$, and note that $r_1 = r_2 =: r$ because of the continuity condition for the wave function at

$x = 0$, we arrive at the form of the wave function given in Section 2.

Appendix B. Explicit coefficients

Setting $r = 1$ we read off from (2)

$$\varrho_1^{(i)} = -\frac{(1+i\gamma)\exp(-2bk_i) + 1 + i\gamma - 2k_i}{(1+i\gamma)\exp(-2bk_i) - 1 - i\gamma + 2k_i} \tag{B.1}$$

$$\varrho_2^{(i)} = +\frac{(1-i\gamma)\exp(-2bk_i) + 1 - i\gamma - 2k_i}{(1-i\gamma)\exp(-2bk_i) - 1 + i\gamma + 2k_i}, \tag{B.2}$$

where a zero k_i, $i = 1, 2, 3$ of the determinant of $\mathcal{M}$ has to be inserted to satisfy the third equation of (2). Note that both denominators vanish at the intermediate (the second) value k_2 for $\gamma \to 0$, i.e. when $b = -\mathrm{Log}(1 - 2k_2)/(2k_2)$. Inserting this expression into $\varrho_1^{(2)}$ and $\varrho_2^{(2)}$ the expansions in powers of γ as given in the main text follow.

Appendix C. Relation to realistic wave guides

Let us assume a wave guide of width a centred around the origin $x = 0$ and placed on a substrate with background refractive index n_0. Across the wave guide the refractive index is altered to $n(x) = n_0 + \Delta\tilde{n}$, where $\Delta\tilde{n}$ is complex, constant, and $|\Delta\tilde{n}| \ll n_0$. The eigenvalue equation of the amplitude of the electric field vector of an electromagnetic wave propagating along the wave guide in the z direction, $\tilde{E}_y(x, z, t) = E_y(x)\mathrm{e}^{i(\beta z - \omega_0 t)}$, with β the propagation constant, reads (*cf.* [5])

$$\left(\frac{\mathrm{d}^2}{\mathrm{d}x^2} + k_0^2 n^2(x)\right) E_y(x) = \beta^2 E_y(x)\ , \tag{C.1}$$

where $k_0 = 2\pi/\lambda_0 = \omega_0/c$, with λ_0 the vacuum wavelength. To first order in $\Delta\tilde{n}$, $n^2(x) = n_0^2 + 2n_0\Delta\tilde{n}$, and (C.1) becomes

$$\left(\frac{\mathrm{d}^2}{\mathrm{d}x^2} + 2n_0\Delta\tilde{n}k_0^2\right) E_y(x) = (\beta^2 - n_0^2k_0^2)E_y(x)\ . \tag{C.2}$$

If we replace the effect of the altered refractive index across the wave guide by a delta function $V_0\delta(x)$ we have to require that the integral across the wave guide obeys $2n_0\Delta\tilde{n}k_0^2\ a = V_0$. Instead of (C.2) we then have

$$\left(\frac{\mathrm{d}^2}{\mathrm{d}x^2} + 2n_0\Delta\tilde{n}k_0^2\ a\ \delta(x)\right) E_y(x) = (\beta^2 - n_0^2k_0^2)E_y(x)\ . \tag{C.3}$$

We decompose $\Delta\tilde{n}$ into its real and imaginary parts, $\Delta\tilde{n} = \Delta n + i\Delta n'$. The characteristic length scale set by Δn is

$$\ell = (2n_0\Delta n k_0^2)^{-1/2}. \tag{C.4}$$

Defining a further length scale $L = \ell^2/a$ and multiplying (C.3) by $-L^2$, by noting that $L\ \delta(x) = \delta(\tilde{x})$, with the dimensionless coordinate $\tilde{x} = x/L$, we finally obtain

$$\left(-\frac{\mathrm{d}^2}{\mathrm{d}\tilde{x}^2} - (1 + i\Delta n'/\Delta n)\ \delta(\tilde{x})\right) E_y(\tilde{x}) = -L^2(\beta^2 - n_0^2k_0^2)E_y(\tilde{x})\ . \tag{C.5}$$

Comparing (C.5) with the triple delta-function Schrödinger equation (1), we identify $\gamma = \Delta n'/\Delta n$, where the eigenvalues of (C.5) are related to the eigenvalues k^2 of (1) by $k^2 = L^2(\beta^2 - n_0^2k_0^2)$, and the dimensionless coordinate x in (1) is equal to $\tilde{x}$.

To give an example, for the values used in [5], $n_0 = 3.3, \Delta n = 10^{-3}$, $\lambda = 1.55$ μm and $a = 5$ μm, one obtains $\ell = 3.036$ μm and $L = 1.843$ μm, both on the order of the wavelength of the injected microwave.

Acknowledgement

WDH and GW gratefully acknowledge the support from the National Institute for Theoretical Physics (NITheP), Western Cape, South Africa. GW expresses his gratitude to the Department of Physics of the University of Stellenbosch where this work was carried out.

References

[1] C. M. Bender and S. Boettcher. Real spectra in non-Hermitian Hamiltonians having $\mathcal{PT}$ symmetry. *Phys. Rev. Lett.*, 80:5243, 1998.

[2] N. Moiseyev. *Non-Hermitian Quantum Mechanics*. Cambridge University Press, Cambridge, 2011.

[3] W. D. Heiss. The physics of exceptional points. *J. Phys. A*, 45:444016, 2012.

[4] C. M. Bender, M. Gianfreda, P. Peng, S. K. Özdemir, and Yang L. Twofold transition in $\mathcal{PT}$-symmetric coupled oscillators. *Phys. Rev. A*, 88:062111, 2013.

[5] Sh. Klaiman, U. Günther, and N. Moiseyev. Visualization of branch points in $\mathcal{PT}$-symmetric waveguides. *Phys. Rev. Lett.*, 101:080402, 2008.

[6] Ch. E. Rüter, K. G. Makris, R. El-Ganainy, D. N. Christodoulides, M. Segev, and D. Kip. Observation of parity-time symmetry in optics. *Nat. Phys.*, 6:192, 2010.

[7] E.-M. Graefe, U. Günther, H. J. Korsch, and A. E. Niederle. A non-Hermitian $\mathcal{PT}$ symmetric Bose-Hubbard model: eigenvalue rings from unfolding higher-order exceptional points. *J. Phys. A*, 41:255206, 2008.

[8] W. D. Heiss. Chirality of wavefunctions for three coalescing levels. *J. Phys. A*, 41:244010, 2008.

[9] G. Demange and E.-M. Graefe. Signatures of three coalescing eigenfunctions. *J. Phys. A*, 45:025303, 2012.

[10] J.-W. Ryu, S.-Y. Lee, and S. W Kim. Analysis of multiple exceptional points related to three interacting eigenmodes in a non-hermitian hamiltonian. *Phys. Rev A*, 85:042101, 2012.

[11] R. Gutöhrlein, J. Main, H. Cartarius, and G. Wunner. Bifurcations and exceptional points in dipolar Bose-Einstein condensates. *J. Phys. A*, 46:305001, 2013.

[12] W. D. Heiss and G. Wunner. Resonance scattering at third-order exceptional points. *J. Phys. A*, 48:345203, 2015.

[13] M. Am-Shallem, R. Kosloff, and N. Moiseyev. Exceptional points for parameter estimation in open quantum systems: Analysis of the Bloch equations. *New Journal of Physics*, 17(11):113036, 2015.

[14] M. Am-Shallem, R. Kosloff, and N. Moiseyev. Parameter estimation in atomic spectroscopy using exceptional points. arXiv:1511.07205v2.

[15] K. Ding, G. Ma, M. Xiao, Z. Q. Zhang, and C. T. Chan. The emergence, coalescence and topological properties of multiple exceptional points and their experimental realization. arXiv:1509.06886.

[16] V. Jakubský and M. Znojil. An explicitly solvable model of the spontaneous $\mathcal{PT}$-symmetry breaking. *Czech. J. Phys.*, 55:1113–1116, 2005.

[17] A. Mostafazadeh. Delta-function potential with a complex coupling. *J. Phys. A*, 39:13495, 2006.

[18] H. Mehri-Dehnavi, A. Mostafazadeh, and A. Batal. Application of pseudo-Hermitian quantum mechanics to a complex scattering potential with point interactions. *J. Phys. A*, 43:145301, 2010.

[19] A. Mostafazadeh. Nonlinear spectral singularities for confined nonlinearities. *Phys. Rev. Lett.*, 2013.

[20] H. F. Jones. Interface between Hermitian and non-Hermitian Hamiltonians in a model calculation. *Phys. Rev. D*, 78:065032, 2008.

[21] H. Cartarius and G. Wunner. Model of a $\mathcal{PT}$-symmetric Bose-Einstein condensate in a δ-function double-well potential. *Phys. Rev. A*, 86:013612, 2012.

[22] H. Cartarius, D. Haag, D. Dast, and G. Wunner. Nonlinear Schrödinger equation for a $\mathcal{PT}$-symmetric delta-function double well. *Journal of Physics A*, 45:444008, 2012.

[23] A. Löhle, H. Cartarius, D. Dast, D. Haag, J. Main, and G. Wunner. Stability of Bose-Einstein condensates in a $\mathcal{PT}$-symmetric double-delta potential close to branch points. *Acta Polytechnica*, 54:133, 2015.

[24] I. V. Barashenkov and D. A. Zezyulin. Localised nonlinear modes in the $\mathcal{PT}$-symmetric double-delta well Gross-Pitaevski equation. arXiv:1511.06599v1.